Extraction and Characterization of Bamboo *Rhipidocladum cf. Harmonicum* (Parodi) McClure Starch

Alexander Puentes Parra[1] · Claudia Elizabeth Mora Huertas[1]*

Received: 5 November 2020 /Accepted: 24 February 2021

Abstract: Starch is a biodegradable and biocompatible polymer recognized as a versatile starting material for pharmaceutical and food products; therefore, the investigation of unconventional sources of this material is always attractive. In this research, bamboo starch was isolated and characterized regarding some of its physical, chemical, and physicochemical properties. Bamboo starch is present in bamboo stems and located in the long cells of the cortical parenchyma; its granules exhibit irregular shape, average size of 15 µm ± 1.0 µm, amylose content of 18.3% ± 1.2%, a crystallographic pattern corresponding to polymorph A with high gelatinization temperature (79.1°C) and low enthalpy (ΔH: 8.8 Jg^{-1}), swelling power and solubility. The bamboo starch characterization suggests its performance as an excipient for pharmaceutics and cosmetics products or as a food ingredient like the more used starches. Besides, the starch extraction yield (22.9% ± 1.0%) and the characteristics of the bamboo crop´s growth and development offer an opportunity to add value to this natural resource by exploiting its starch.

Keywords: Bamboo, microscopy, starch, thermal properties, X-ray diffraction

*Corresponding Author

[1] Universidad Nacional de Colombia, Sede Bogotá. Facultad de Ciencias. Departamento de Farmacia. Carrera 30 45-03, edificio 450, Bogotá, Tel: +5713165000 ext. 14609, codigo postal 111321, Colombia
E-mail: cemorah@unal.edu.co

Published online 2 August 2021

Introduction

Starch is a non-structural carbohydrate, insoluble in water, composed of two homopolymers with D-glucose units known as amylose and amylopectin, representing around 98% of its weight on a dry basis and whose ratio varies according to the botanical source (Tester *et al*., 2004). In plants, starch exists as insoluble semicrystalline granules biosynthesized, for example, in leaves, roots, shoots, fruits, grains, and stems (Bertoft, 2017; Preiss, 2018). The ratio amylose/amylopectin and how they organize within the granules vary within and between the different species, affecting starch properties such as the granule shape and size, water absorption, swelling, gelling, and susceptibility to enzymatic degradation, among others (Wang and Copeland, 2013). This variability originates mainly in biosynthetic processes since genes subject to developmental controls and environmental influences are involved (Wang and Copeland, 2013). Likewise, the starch isolation method and the analytical techniques used for its characterization are factors explaining such variability (Vamadevan and Bertoft, 2015).

Most native starches characterize by an amylose content vary between 20% and 30%, although natural variants may be outside this range (Chung and Liu, 2009; Wang and Copeland, 2013). On the other hand, starch granules can contain small amounts of proteins located at the surface level, as well as minerals and lipids (Vamadevan and Bertoft, 2015). The latter represents the most

important associated fraction in starch granules; thus, in some cereal starches such as wheat, there are percentages between 0.8% and 1.2%, and for corn starch, between 0.6% and 0.8% (Buléon *et al*., 1998). Some starch granules contain pores on the surface and internal channels that vary in terms of their location, dimension, and extension and that could be connected between themselves and with the internal cavity of the granule as occurs in corn and sorghum starches (Jane, 2009; Qi and Tester, 2019).

Commercially available starches are isolated mainly from cereals such as corn and wheat and tubers such as potatoes and tapioca, with corn being the most important source with a world production higher than 80% (Lawton, 2016). Among starch applications as an excipient in the pharmaceutical industry, its use as a diluent, disintegrant, binder, absorbent, and stabilizing agent, is highlighted (Qi and Tester, 2019). Likewise, starches have been investigated as carriers of active molecules providing innovative solutions to reduce their side effects and protect them against adverse environmental or physiological conditions (Mateescu *et al*., 2015). Besides, drug-starch complexes could allow targeted and modified delivery (Marinopoulou *et al*., 2019), meeting the requirements of biodegradability and biocompatibility. For this purpose, encapsulation techniques have been developed using starches such as spray drying (Ocampo-Salinas *et al*., 2020; Rocha *et al*., 2012), extrusion (Xie *et al*., 2020), fluidized bed coating (Li *et al*., 2019), and coacervation (Albert *et al*., 2019; Saifullah *et al*., 2019; Waterschoot *et al*., 2015) among other. Likewise, starch has become a starting material to develop excipients with new functionalities, as is the case of modified starches used to prepare Pickering emulsions (Albert *et al*., 2019). In the food industry, starch acts as moisture retention, texturizing, thickening, gelling, film-forming, and adhesive agent. In the same way, it is a source of sweetening syrups such as glucose, fructose, mannitol, sorbitol, and maltitol (Waterschoot *et al*., 2015). On the other hand, starch is used in paper production as a flocculant and retention aid, as a binder for coatings, and as an adhesive in corrugated cardboard and laminates, among others (Maurer, 2009).

The different starch properties due especially to the botanical source, motivate the exploration of new sources of this carbohydrate. Thus, this research work aims to explore bamboo as a non-conventional source of starch, characterizing some of its general properties such as morphology, particle size, amylose content, type of polymorph, and gelatinization behavior, among others. The global bamboo market was valued at 3.600 million USD at the end of 2017 (Chen *et al*., 2020) thanks to its use as a construction material since ancient times (Hong *et al*., 2020) and as an inexpensive, ecological, and sustainable substitute for wood. On the other hand, bamboo culms are marketed as food products given their sweet character and their content of phytosterols, vitamins A, B6, C, and E, and 17 amino acids, of which eight are essential for the human body (Felisberto *et al*., 2016). Besides, bamboo´s high fiber content makes it a source for dietary fiber extraction (Felisberto *et al*., 2017). From an agricultural standpoint, the bamboo crop does not require pesticides and has no history of spreading pests, unlike soybean, corn, wheat, or sugar cane crops. Additionally, it is an economically viable crop non requiring recultivation processes because its perennial and asexual culms (Felisberto *et al*., 2017). Also, bamboo has a growth of approximately 36 m in 6 months (Luo *et al*., 2019) and high production of biomass (7 - 39 t/ha per year) (Kuehl, 2015) to obtain biofuels (Littlewood *et al*., 2013).

Materials and Methods

Bamboo culms of 10 - 12 years-old were collected in Garagoa, Boyacá, Colombia (5°04'56"N 73°21'50"W, elevation: 1685 m.a.s.l.) and identified as *Rhipidocladum cf. Harmonicum* (Parodi) McClure, Poaceae family (National Herbarium of Colombia, Universidad Nacional de Colombia, collection-number 610329). To identify the starch granules within the bamboo structure, some samples of the material were observed by scanning electron microscopy (FEI Quanta 200, operated under vacuum at a pressure of 5.3 x 10^{-5} Pa and acceleration energy of the electron beam of 30 kV).

Solvents as ethanol (96%), acetone, ethyl acetate, methanol, and DMSO were obtained from Merck

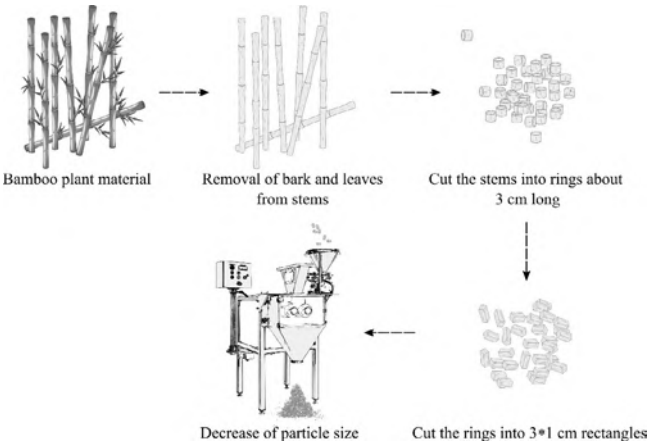

Fig 1. Steps for the pretreatment of vegetal bamboo material before starch extraction

Millipore. Sodium azide (NaN_3) and potato amylose standard (A0512) were purchased from Sigma-Aldrich. Potato amylopectin standard (10118) was obtained from Fluka Biochemika. All other chemical reagents were analytical grade and distilled water obtained from a Boeco WS 8000 system, was used in all cases.

Extraction of Bamboo Starch

Bamboo as vegetal material was pretreated by manual removal of the leaves and bark from the stems (fig. 1). Then, the stems were cut with an industrial saw to obtain particles of approximately 3 x 1 x 1 cm and milled (Erweka KU1) until a fine powder. For the starch extraction (fig. 2), 200 mL of a 1% w/v NaCl solution at 4°C and 100g of the powder material obtained were mixed for 60s (Vitamix 62825 industrial blender) to promote the disintegration of the stems cortical parenchyma and allow the granules release (Cailliau *et al.*, 2007). The suspension obtained was filtered using a cloth filter and the retained material was subjected to the same mixing procedure as necessary until no starch was detected in the filtrate, which was verified by a qualitative test using an iodine-potassium iodide solution ($2.5x10^{-3}$ M I_2 / $6.5x10^{-3}$ M KI). The filtrates obtained were collected in glass bottles stored at 4°C, and the starch was settled by gravity for 18h. NaN_3 (20 ppm) was used as a preservative to avoid any biological fermentation process caused by microbial activity. After 18h, the sedimented material was washed three times, discarding the supernatant and resuspending the sediment in distilled water. Finally, the starch obtained was filtered under vacuum (Vacuum Pump R-400), washed three times with ethanol (96%), and finally with acetone; then it was dried at 45°C ± 2°C (Jouan IG 150) for 12h until constant weight (Ohaus™ PA214). The solid material cake was crushed with a mortar and stored in hermetically sealed glass containers for later characterization and use.

Characterization of Bamboo Starch

Starch Morphology: The starch samples were dispersed in distilled water and sonicated (Elma S15H bath) for 1 min at a frequency of 37 kHz to favor their dispersion. A drop of the starch dispersion was then placed on a slide and covered with a coverslip slide for observation in an optical microscope (Olympus™ BX51-P) in normal and polarized light mode. Likewise, the starch´s scanning electron micrographs were taken (scanning electron microscope FEI Quanta 200; vacuum at a pressure of 5.3 x 10^{-5} Pa and acceleration energy of the electron beam of 30 kV). The starch samples were coated with 99.9% pure gold, using a rotary pump sputter coater (Q150R ES) for 30s at a spray current of 60 mA.

Particle size and size distribution: To this end, the laser diffraction technique (Mastersizer 3000, Malvern) operated in general mode with the Mie dispersion model, was used with the following conditions: 20 mg of starch (refractive index: 1.52, absorption index: 0.18, density: 1 g/cm^3, particle type: non-spherical); dispersant: water 500 mL; darkening: between 5% and 6%;

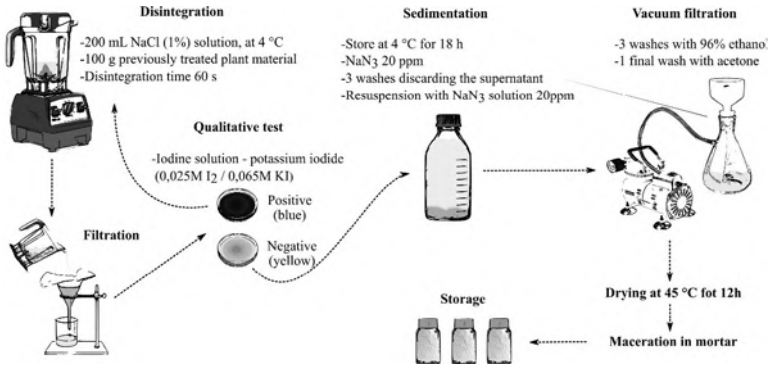

Fig 2. Steps for extracting starch from bamboo culms

background measurement duration: 60s; sample measurement duration: 60s; background stability assessment: 180s; stirring rate: 2100 rpm, ultrasound: 1200s at 100%; degassing and alignment after ultrasound; number of measurements: 5.

Moisture content: Thermogravimetric method using a halogen moisture analyzer (Radwag™ PMX 50). The moisture content was reported as a percentage of the initial weight of the sample.

Ashes: AOAC 923.03 method (AOAC, 2003), starch samples (2g) deposited in porcelain crucibles and, subsequently placed in a muffle at a temperature of 600°C for 3h.

Lipids content: AOAC 945.16 method (AOAC, 2003). The percentage of lipids in the starch sample was determined by extraction with organic solvents using Soxhlet equipment. For this purpose, 30g of sample was deposited in an extraction thimble and refluxed for 8h using 200 mL of a mixture of ethyl acetate - methanol (1:1). Subsequently, the solvents were evaporated with a rotary evaporator (Heidolph Hei-VAP, 60°C, 200 mbar, and 80 rpm). The remaining material was extracted with acetone and dried in an oven (Jouan IG 150) for 12h at 45°C until constant weight. The lipids content was reported as a percentage of the initial weight of the sample.

Crude fiber content: AOAC 962.09 method (AOAC, 2003). For the determination of crude fiber, 3g of starch were digested with a 0.1 N KOH solution (300 mL) at 90°C (IKA™ C-Mag HS 7) for 4h with continuous stirring (250 rpm). Subsequently, the solution was filtered under vacuum (vacuum pump R-400) while hot, the residue was washed twice with distilled water and dried in an oven (Jouan IG 150) at 45°C for 24h until constant weight. The crude fiber content was reported as a percentage of the initial weight of the sample.

Amylose content: The amylose content was spectrophotometrically measured following the procedure described by McGrance *et al*., (1998) with slight modifications. Initially, a calibration curve with six levels of amylose - amylopectin ratio (0:100; 10:90; 25:75; 50:50; 75:25; and 100:0) was prepared using potato amylose and potato amylopectin standards previously dried (oven Jouan IG 150) for 12h at 45°C, up to constant weight. Thus, 20 mg of the corresponding amylose - amylopectin mixture was dispersed in 6 mL of DMSO using hermetically sealed glass vials. This mixture was heated for 1h at 90°C (IKA™ C-Mag HS 7) in a water bath under continuous stirring (250 rpm); the samples were cooled to room temperature and the solution obtained was completed to a total volume of 10 mL using distilled water. Then, 500 µL of that dilution were diluted with water to a total volume of 25 mL. The mixture amylose – amylopectin 100:0 was chosen to determine the amount of iodine - potassium iodide solution (2.5×10^{-3} M I_2 / 6.5×10^{-3} M KI) necessary for the analysis, i.e., the amount in which the absorbance of the sample is not affected since the complete complexation of iodine with amylose is guaranteed. Thus, 1.4 mL of the amylose solution were deposited in 1.5 mL Eppendorf tubes and a specific volume of the iodine - potassium iodide solution (40, 60, 80, and 100 µL) was added, it was vortexed (LB PRO MX-S) for 1 min and left to stand for 15 min for further analysis. The absorbance

spectra were taken in a range of 250 nm to 950 nm (UV-Vis spectrophotometer Shimadzu UV-1800) using quartz cells with a length of 1 cm, a mean scanning speed, and a sampling interval of 0.5 nm. Distilled water was used as a blank. According to the spectra obtained, it was concluded that the necessary amount of iodine for the determination of amylose in starch was 100 µL and that the most suitable wavelength corresponded to 620 nm. The procedure previously described for elaborating the calibration curve was followed to determine the starch sample´s amylose content. Measurements were carried out in triplicate.

High-pressure differential scanning calorimetry (HP-DSC): The glass transition temperature and its enthalpy were determined in a high-pressure calorimeter (HP DSC1 Mettler Toledo™), previously calibrated with indium and palladium standards. Thus, 1 mg of sample was weighed into standard aluminum crucibles (capacity: 40 µL) and 5 µL of distilled water were added; the crucibles were hermetically sealed, and a small hole was made in the lid. The equipment was operated under a nitrogen atmosphere at a pressure of 1 Mpa, heating rate: 10°C/min, temperature range: 25°C to 130°C, an empty crucible was used as a reference. Data treatment was performed using STARe software; graphs and treatment for the baseline were performed with OriginPro™ 9 software.

Fourier transform infrared spectroscopy (FTIR): The vibrational spectra were taken in a spectrophotometer (IR-Affinity-1S SHIMADZU) equipped with an ATR accessory; scanning range: 3500 cm^{-1} to 400 cm^{-1}, resolution: 4 cm^{-1}. The graphs and treatment for the baseline were carried out with the OriginPro™ 9 software.

X-ray diffraction (XRD): The crystallographic pattern of starch was determined in a PANalytical X'PERT PRO MPD X-ray diffractometer, Bragg-Brentano optical configuration, equipped with a high-speed solid-state detector (PIXcel) and an X-ray generator tube with a copper anode. Measurement conditions: wavelength 1.54 Å, nickel filter, voltage 45 Kv, current 40 mA, scanning region with two theta (2θ) angle from 7° to 100°, step size 0.0263°, step time 100s. The percentage of relative crystallinity was determined by the ratio of the crystalline areas and the total area corresponding to the crystalline areas plus the amorphous areas´ contribution, following the procedure described by Lopez-Rubio *et al*., (2008). Data treatment and curve fitting was performed using the HighScore Plus software (version 3.0c) with a Gaussian function.

Swelling power and solubility: As proposed by Li and Yeh (2001), 100 mg of sample were deposited in 50 mL Falcon tubes previously weighed, 10 mL of distilled water were added, and they were hermetically sealed and heated for 1h under continuous stirring (250 rpm) in a water bath at different temperatures: 50°C, 60°C, 70°C, 80°C, and 90°C (IKA™ C-Mag HS 7). The solution was cooled to room temperature and centrifuged at 8000 rcf for 20 min (Thermo Scientific™ Heraeus Megafuge 16), the supernatant was carefully separated from the sediment, poured onto previously weighed Petri dishes, and dried until the water evaporation (IKA™ oven 125 at 100°C); the residual material corresponds to soluble starch. The sediment dry weight was determined after drying under the same conditions previously mentioned. The swelling power and insoluble solids correspond to the percentages of soluble starch and dry sediment with respect to the initial weight of the sample, respectively.

Results and Discussion

The bamboo characterizes by short and long parenchyma cells positioned vertically; the long cells exhibit thick, polylamellar, and lignified walls where the starch granules are located, and the short parenchyma cells are scattered among long cells having thin walls, dense cytoplasm, and evidence of peroxidase enzyme activity (He *et al*., 2002). fig.3 shows the location of the starch granules in the bamboo stems used in this research work and, as can be seen, the walls of the parenchyma have small holes that play an essential role in the flow of raw sap from the root to the leaves of the plant (Luo *et al*., 2019).

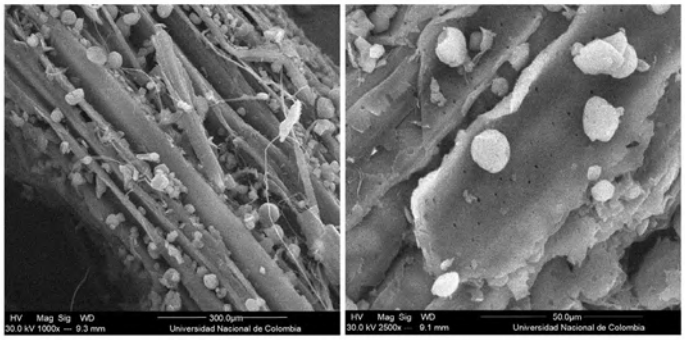

Fig 3. Scanning electron micrographs of cell parenchyma in bamboo fibers

The starch extraction yield was 22.9% ± 1.0% on a dry basis, excluding moisture and the percentages of lipids, ash, and fiber (Table 1). This yield is considered high compared to the values reported when starch was extracted from different bamboo species. For example, Felisberto *et al*., (2018) report extraction percentages of 11.6%, 15.2%, and 14.6% corresponding to the lower, middle, and upper part, respectively, of a three-year-old bamboo culm (*Dendrocalamus asper*). For their part, Toledo *et al*., (1987) report an extraction percentage of 8.5% for the bamboo species *Guadua flabellata*. These differences in the amount of starch extracted could be attributed to the procedure used for the extraction. Likewise, the plant´s age, botanical differences, and climatic and geological conditions of the region where bamboo is cultivated could significantly affect the starch content (Asaoka *et al*., 1984,1985,1989). In this sense, it has been found that bamboo culms *Phyllostachys viridiglaucescens* do not contain starch during the growth phase because all the nutrients of the plant must be used immediately for its metabolic processes and, in older culms, starch is present even up to 12 years (Liese and Weiner, 1996).

Likewise, the extraction yield of starch from the investigated bamboo was higher than those reported values for conventional sources of starch, such as bean (between 16.4% and 22.2%) (Ngobese *et al*., 2018; Hoover *et al*., 2010; Tjahjadi and Breene, 1984), sweet potato (12.9% and 22.8%) (Rahman *et al*., 2003; Moorthy, 1991), and cassava (21.8%)

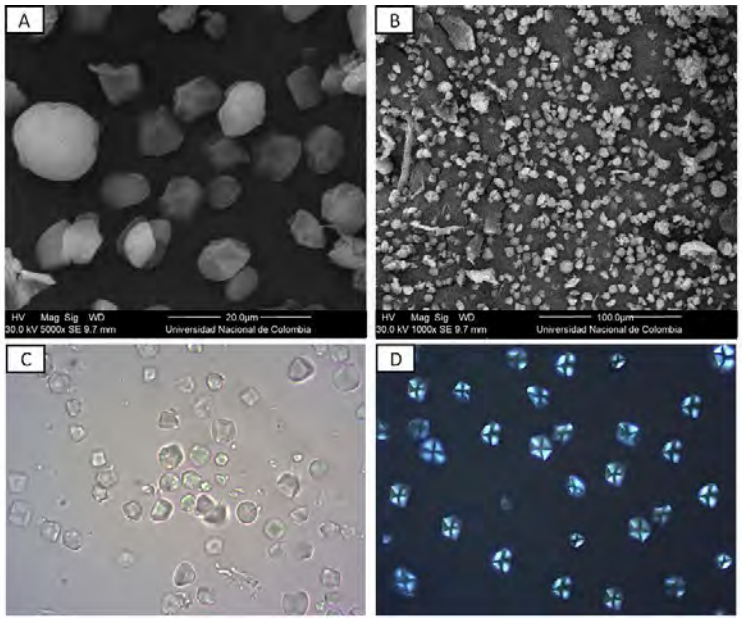

Fig 4. Micrographs of the granules of bamboo starch, observed by scanning electron microscopy (A and B); optical microscopy without polarized light with a magnification of 100x (C); polarized light optical microscopy with a magnification of 100x (D)

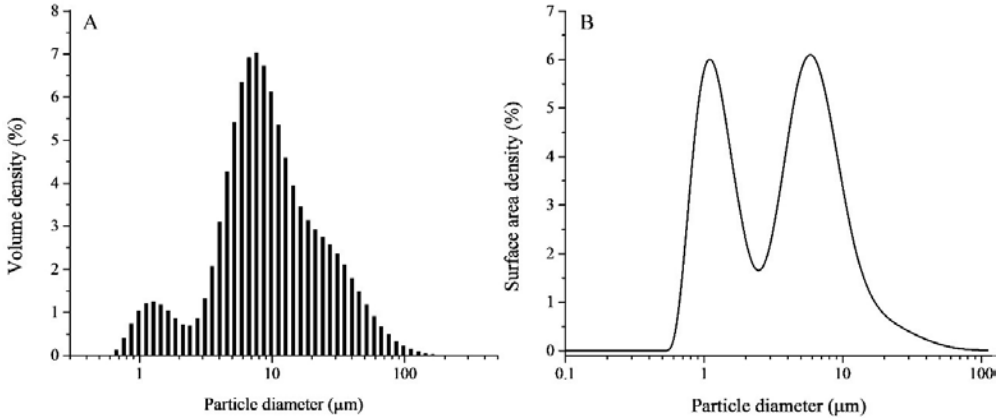

Fig 5. Volume density distribution of the particle size of bamboo starch (A); particle size distribution of bamboo starch in terms of surface area (B)

(Moorthy, 1991). Nevertheless, other conventional sources of starch characterize by better yields compared with bamboo. Such is the case with corn (between 45.0% and 75.8%) (Ji *et al*., 2004; Mistry *et al*., 1992; Núñez-Bretón *et al*., 2019), rice (44.0% and 64.4%) (Ramos da Silva *et al*., 2020; Hoover *et al*., 1996), pea (35%) (Ngobese *et al*., 2018) and oat (23.4%) (Hoover and Vasanthan, 1992).

On the other hand, the apparent content of amylose present in bamboo starch was 18.3% ± 1.2%, which is characteristic of native starches and is in the range between 12% and 30% reported for other bamboo species (Ai *et al*., 2016; Felisberto *et al*., 2018; Toledo *et al*., 1987).

Fig. 4A shows that bamboo starch granules exhibit irregular shapes, some of them with polyhedral edges. This morphology is similar to that for bamboo species such as *Dendrocalamus asper* (Felisberto *et al*., 2018), *Guadua flabellate* (Toledo *et al*., 1987), and bamboo seeds from *Phyllostachys heterocycle var. pubescens* (Mazel) ohwi (Ai *et al*., 2016). These irregular granule shapes have also been reported for starches extracted from normal and waxy corn (Jane, 2009).

As the starches isolated from other sources included in the Poaceae family, such as rice, corn, sorghum, barley, and wheat, bamboo starch characterizes by compound granules formed by the assembly of several simple granules present in the amyloplast; this is a resource that the plant uses during the starch biosynthesis, possibly to achieve greater storage (Matsushima *et al*., 2015). Besides, the presence of some impurities (fig. 4B and 4C), mainly due to fibers remaining from the extraction process, is evident and consistent with the high fiber content determined in the chemical analysis (Table 1). Observations of the bamboo starch granules by polarized light (fig. 4D) evidence birefringence inherent to their semicrystalline regions and confirm the integrity of the starch´s macroscopic structure, i.e., the extraction process does not alter the granule structure.

On the other hand, to estimate the particle size distribution of bamboo starch, initially, its refractive and absorption indices were determined by using a simulator for optimizing the optical properties of the material, included in the V3.62 software and the graph data and adjustment. Data obtained from the measurement and data predicted by the model are superimposed, and their adjustment is verified through the value of the residuals (Beekman *et al*., 2005). The suitability of the estimated refractive and absorption indices was demonstrated by comparing the theoretical and real concentrations of the suspended particles in the dispersant through the extinction coefficient measured by the equipment according to the Mie theory of light scattering and the Lambert-Beer theory. In this case, the difference between the two concentrations must be a maximum of 20%, much higher than the value of 0.0003% obtained in this research (Beekman *et al*., 2005).

As shown in fig. 5A, bamboo starch exhibits a bimodal particle size distribution with small sizes in the range between 0.6 μm and 2.5 μm and large

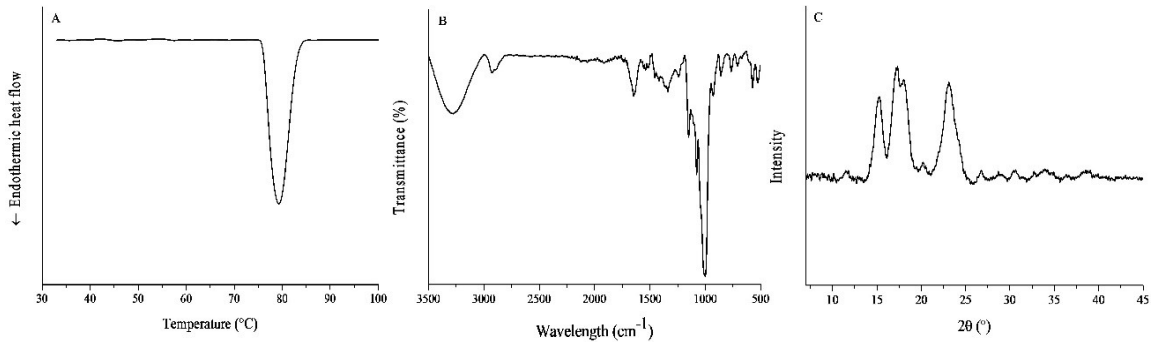

Fig 6. Thermogram obtained for bamboo starch by HP-DSC (A); infrared spectrum obtained for bamboo starch (B); X-ray diffraction pattern of bamboo starch (C)

sizes between 2.5 µm and 100 µm, data that can be observed with greater clarity in terms of surface area (fig. 5B). Consistent with the observations by scanning electron microscopy (fig. 4), particle sizes smaller than 1 µm could be attributed to tiny starch granules or small fiber fragments remaining from the extraction process, since the analysis cannot discriminate between particles of starch and some irregular impurities that the model assumes as spheres, within the concept of equivalent spheres. In the same line, particle sizes greater than 36 µm might correspond to fibers present in the starch or aggregates of granules; therefore, sonication and shaking are essential during the particle size measurement. However, as seen in fig. 5A, these particle size distributions have volume density percentages below 1.5%, which indicates that only 1.5% of the total volume measured comes from those particle diameters and the most significant contribution to the total volume corresponds to the particle diameters between ~3.6 µm and ~ 36 µm.

Accordingly, the most useful data to represent the range of particle sizes of bamboo starch were D10 and D90, which correspond to the diameters from which 10% and 90% of the particle population is below, respectively. Thus, the bamboo starch characterizes by a volume size distribution in the range of 3.1 µm ± 0.1 µm to 34.4 µm ± 2.1 µm with a coefficient of variation of 3% and 4%, respectively, which suggest reproducibility of the measurements as established in the ISO 13320-1

Table 1. Chemical and physicochemical characteristics obtained for bamboo starch

Test		Result
Chemical characterization	Moisture† (%)	5.5 ± 1.7
	Ash† (%)	0.1 ± 0.1
	Fiber (%)	9.7 ± 0.2
	Lipids† (%)	0.2 ± 0.1
	Amylose† (%)	18.3 ± 1.2
X-ray diffraction	Crystallographic pattern	Type A
	Crystallinity (%)	21.7
Thermal properties	To (°C)	75.8
	Tp (°C)	79.1
	Tc (°C)	82.9
	ΔH (J.g-1)	8.8

† Data reported as the mean ± confidence interval of 3 replicates; gelatinization enthalpy (ΔH); onset temperature (To); peak temperature (Tp); conclusion temperature (Tc); gelatinization enthalpy (ΔH).

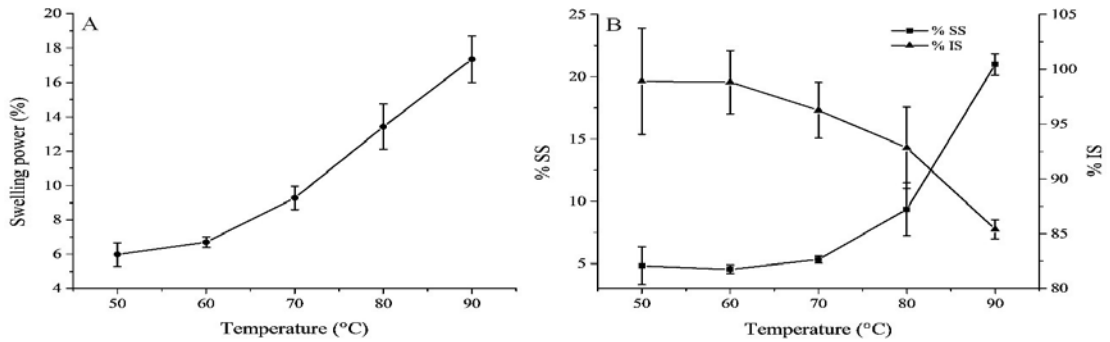

Fig 7. Swelling power of bamboo starch (A); percentage of soluble solids (%SS) and insoluble (%IS) leached in bamboo starch (B)

standard included in the equipment software (Mastersizer v3.62). Besides, unique values of the particle size such as the De Brouckere mean diameter (D4,3), the Sauter mean value (D3,2), the median (D50), and the span value were calculated. Thus, the bamboo starch has a mean diameter D4,3 of 15.0 µm ± 1.0 µm in terms of volume; when the distribution is analyzed in terms of surface area, the mean value D3,2, which is sensitive to the presence of fine particles in the size distribution, is 6.0 µm ± 0.1 µm. The median D50, which corresponds to the mean value from which half of the population resides both above and below this value, was 9.3 µm ± 0.4 µm. Finally, the span was 3.4, a high value that suggests a wide distribution, that is, little homogeneity of the sample.

On the other hand, bamboo starch has a high gelatinization temperature and low gelatinization enthalpy (Table 1, fig. 6A) compared with starches from other botanical sources such as corn and potatoes, whose gelatinization temperatures and enthalpies vary between 62.5°C and 71°C, and between 11.07 $J.g^{-1}$ and 19.8 $J.g^{-1}$, respectively (Alvani *et al*., 2011; Jiang *et al*., 2020; Rocha *et al*., 2011; Srichuwong *et al*., 2005). This could be related to the characteristics of the branched chains of amylopectin, where the stable double helix chains could favor the packaging of the amylopectin chains in crystalline regions. This could confer thermal stability to these structures, as proposed by Felisberto *et al*., (2018) for the *Dendrocalamus asper* bamboo starch and by Ai *et al*., (2016) for the starch from bamboo seeds (*Phyllostachys heterocycle var. pubescens* (Mazel) ohwi), whose gelatinization temperatures and enthalpies were between 73.4°C and 84°C and 4.2 $J.g^{-1}$ and 14.2 $J.g^{-1}$, respectively.

The FTIR spectrum of bamboo starch is shown in fig. 6B. The characteristic peaks for the -OH groups of the glucose residues and the water present in the sample appear at ~3280 cm^{-1} and at ~1648 cm^{-1}, which are assigned to stretching and bending vibrations, respectively. The stretching vibration for the C-O bond appears at ~1150 cm^{-1}, C-O-C at ~997 cm^{-1}, and C-O-H at ~1078 cm^{-1}. The stretching vibration corresponding to the C-H bond is observed at ~2930 cm^{-1}.

The XRD pattern of the investigated bamboo starch is shown in Fig. 6C. As can be seen, this starch exhibits a type A crystalline pattern (orthogonal unit cell with slightly distorted hexagonal; a =11.90 Å, b = 17.70 Å, c = 10.52 Å, $\alpha = \beta = \gamma = 90°$) (Sarko and Wu, 1978) with characteristic peaks at Bragg angles (2θ) of 15.3°, 17.2°, 18.1°, and 23°, observations that are consistent with that previously reported by Felisberto *et al*., (2018) for bamboo starch from *Dendrocalamus asper*. According to Tian *et al*., (2010) and Ye *et al*., (2018), the diffraction peak at the 2θ angle of ~20° could be attributed to an endogenous crystal structure of the V-amylose type associated with the presence of amylose-lipid complexes. The type A crystallinity pattern is characteristic of cereal starches such as rice (Bertoft *et al*., 2008; Kong *et al*., 2015; Srichuwong *et al*., 2005), corn (Cheetham and Tao, 1998; Jiang *et al*., 2020; Ngobese *et al*., 2018), rye, wheat, and barley (Ao and Jane, 2007; Bertoft *et al*., 2008), among others. It is important to note that although in these cereals the starch is extracted from a granule and the bamboo from a culm, they belong to the same Poaceae family, which could explain the relationship in the type crystallographic pattern. Similarly, the starch extracted

from genus such as Manioh, Ipomea, Dioscorea, Colocasia, and Coleus also present this type of crystallinity (Gallant *et al*., 1982). The bamboo starch´s crystallographic pattern gives clues about the distribution of its branched amylopectin chains. In this sense, the structure probably corresponds to polymorph A, characterized by having a degree of polymerization (DP) ≥ 37, a low proportion of long chains with a DP of 25 – 36, and a high proportion of short chains with DP of 6 - 12 (Felisberto *et al*., 2018).

The starch swelling behavior is related to its gelatinization and mainly attributed to amylopectin; thus, its value varies inversely with the amylose content (Cozzolino *et al*., 2013). As shown in fig. 7A, the bamboo starch´s swelling power increases with temperature showing the highest values in the region of 70°C to 90°C. Similar behavior is observed for the soluble solids or the solubility index (fig. 7B), which corresponds to the dry matter percentage in the supernatant, mainly amylose. In this case, the soluble solids leached increase significantly in the range between 80°C and 90°C. At this point, the starch structure undergoes an order-disorder transition that breaks down the granule allowing the complete leaching of its components (Hoover, 2001). Regarding insoluble solids (fig. 7B), which refers to the percentage of dry matter in the sediment, as expected, it decreases as a function of the temperature because part of the amylose in the granule has been leached.

Conclusion

This research work contributes to Create an added value to a non-conventional native source of starch as the bamboo (*Rhipidocladum cf. harmonicum* (Parodi) McClure). The extraction yield (22.9% ± 1.0%), its growth habit, and its high biomass production per unit area are attractive for its industrial harnessing. Bamboo starch characterizes by an irregular morphology, mostly granules with polyhedral edges and some of them grouped into compound granules, a type-A X-ray diffraction pattern similar to cereal starches, with a crystallinity percentage of 21.7%, a percentage of amylose of 18.3% ± 1.2%, and a high gelatinization temperature (79.1°C). These findings encourage additional investigations looking for potentialities to develop pharmaceutical, cosmetic, and food products.

Acknowledgement

Authors gratefully acknowledge the "División de Investigación Bogotá" (DIB). Universidad Nacional de Colombia, grant 36019.

References

Adjei, F.K., Osei, Y.A., Kuntworbe, N. and Fori-Kwakye, K. 2017. Evaluation of the disintegrant properties of native starches of five new cassava varieties in paracetamol tablet formulations. *Journal of Pharmaceutics* 2017: 1-9.

Ai, Y., Gong, L., Reed, M., Huang, J., Zhang, Y. and Jane, J. 2016. Characterization of starch from bamboo seeds. *Starch* 68(1–2): 131–139.

Albert, C., Beladjine, M., Tsapis, N., Fattal, E., Agnely, F. and Huang, N. 2019. Pickering emulsions: Preparation processes, key parameters governing their properties and potential for pharmaceutical applications. *Journal of Controlled Release* 309(July): 302–332.

Alvani, K., Qi, X., Tester, R.F. and Snape, C.E. 2011. Physico-chemical properties of potato starches. *Food Chemistry* 125(3): 958–965.

Ao, Z. and Jane, J. 2007. Characterization and modeling of the A- and B-granule starches of wheat, triticale, and barley. *Carbohydrate Polymers* 67(1): 46–55.

Asaoka, M., Okuno, K., Sugimoto, Y., Kawakami, J. and Fuwa, H. 1984. Effect of environmental temperature during development of rice plants on some properties of endosperm starch. *Starch* 36(6): 189–193.

Asaoka, M., Okuno, K. and Fuwa, H. 1985. Effect of environmental temperature at the milky stage on amylose content and fine structure of amylopectin of waxy and nonwaxy endosperm starches of rice (Oryza sativa L.). *Agricultural and Biological Chemistry* 49(2): 373–379.

Asaoka, M., Okuno, K., Hara, K., Oba, M. and Fuwa, H. 1989. Effects of environmental temperature at the early developmental stage of seeds on the

characteristics of endosperm starches of rice (Oryza sativa L.). *Journal of the Japanese Society of Starch Science* 36(1): 1–8.

Association of Official Analytical Chemists (AOAC). 2003. *Official methods of analysis* (17th ed.).

Beekman, A., Shan, D., Ali, A., Dai, W., Ward-Smith, S. and Goldenberg, M. 2005. Micrometer-scale particle sizing by laser diffraction: Critical impact of the imaginary component of refractive index. *Pharmaceutical Research* 22(4): 518–522.

Bertoft, E. 2017. Understanding starch structure: Recent progress. *Agronomy* 7(3): 56.

Bertoft, E., Piyachomkwan, K., Chatakanonda, P. and Sriroth, K. 2008. Internal unit chain composition in amylopectins. *Carbohydrate Polymers* 74(3): 527–543.

Buléon, A., Colonna, P., Planchot, V. and Ball, S. 1998. Starch granules: Structure and biosynthesis. *International Journal of Biological Macromolecules* 23(2): 85–112.

Cailliau, J., Vézina, G., Fortin, F. and Batigne, S. 2007. *The visual guide to understanding plants & the vegetable kingdom* (I. QA (ed.)). Jacques Fortin.

Cheetham, N.W.H. and Tao, L. 1998. Variation in crystalline type with amylose content in maize starch granules: An X-ray powder diffraction study. *Carbohydrate Polymers* 36(4): 277–284.

Chen, M., Ye, L., Li, H., Wang, G., Chen, Q., Fang, C., Dai, C. and Fei, B. 2020. Flexural strength and ductility of moso bamboo. *Construction and Building Materials* 246: 118418.

Chung, H.J. and Liu, Q. 2009. Impact of molecular structure of amylopectin and amylose on amylose chain association during cooling. *Carbohydrate Polymers* 77(4): 807–815.

Cozzolino, D., Roumeliotis, S. and Eglinton, J. 2013. Relationships between swelling power, water solubility and near-infrared spectra in whole grain barley: A feasibility study. *Food and Bioprocess Technology* 6(10): 2732–2738.

Felisberto, M.H.F., Beraldo, A.L. and Clerici, M.T.P.S. 2016. Young bamboo culm flour of *Dendrocalamus asper*: Technological properties for food applications. LWT - *Food Science and Technology* 76: 230–235.

Felisberto, M.H.F., Beraldo, A.L., Costa, M.S., Boas, F.V., Franco, C.M.L. and Clerici, M.T.P.S. 2018. Characterization of young bamboo culm starch from *Dendrocalamus asper*. *Food Research International* 124: 222-229.

Felisberto, M.H.F., Miyake, P.S.E., Beraldo, A.L. and Clerici, M.T.P.S. 2017. Young bamboo culm: Potential food as source of fiber and starch. *Food Research International* 101: 96–102.

Fiedler, J.O., Carmona, Ó.G., Carmona, C.G., José Lis, M., Plath, A.M.S., Samulewski, R.B. and Bezerra, F.M. 2020. Application of *Aloe vera* microcapsules in cotton nonwovens to obtain biofunctional textiles. *Journal of the Textile Institute* 111(1): 68–74.

Gallant, D.J., Bewa, H., Buy, Q.H., Bouchet, B., Szylit, O. and Sealy, L. 1982. On ultrastructural and nutritional aspects of some tropical tuber starches. *Starch* 34(8): 255–262.

He, X.-Q., Suzuki, K., Kitamura, S., Lin, J.-X., Cui, K.-M. and Itoh, T. 2002. Toward understanding the different function of two types of parenchyma cells in bamboo culms. *Plant and Cell Physiology* 43(2): 186–195.

Hong, C., Li, H., Xiong, Z., Lorenzo, R., Corbi, I., Corbi, O., Wei, D., Yuan, C., Yang, D. and Zhang, H. 2020. Review of connections for engineered bamboo structures. *Journal of Building Engineering* 30: 101324.

Hoover, R., Hughes, T., Chung, H.J. and Liu, Q. 2010. Composition, molecular structure, properties, and modification of pulse starches: A review. *Food Research International* 43(2): 399-413.

Hoover, R. 2001. Composition, molecular structure, and physicochemical properties of tuber and root starches: A review. *Carbohydrate Polymers* 45(3): 253–267.

Hoover, R., Sailaja, Y. And *Sosulski*, F.W. 1996. Characterization of starches from wild and long grain brown rice. *Food Research International* 29(2): 99-107.

Hoover, R. and Vasanthan, T. 1992. Studies on isolation and characterization of starch from oat (*Avena nuda*) grains. *Carbohydrate Polymers* 19(4): 285-297.

Jane, J. 2009. Structural features of starch granules II. In B. James and R. Whistler (Eds.), *Starch* (3rd ed., pp. 193–236). Academic Press.

Ji, Y., Seetharaman, K. and White, P.J. 2004. Optimizing a small scale corn starch extraction method for use in the laboratory. *Cereal Chemistry* 81(1): 55-58.

Jiang, F., Du, C., Guo, Y., Fu, J., Jiang, W. and Du, S. 2020. Physicochemical and structural properties of starches isolated from quinoa varieties. *Food Hydrocolloids* 101: 105515.

Kong, X., Zhu, P., Sui, Z. and Bao, J. 2015. Physicochemical properties of starches from diverse rice cultivars varying in apparent amylose content and gelatinisation temperature combinations. *Food Chemistry* 172: 433–440.

Kuehl, Y. 2015. Resources, yield, and volume of bamboos. In Walter Liese and M. Köhl (Eds.), *Bamboo: The Plant and its Uses* (pp. 91–111). Springer International Publishing.

Lawton (Retired), J.W. 2016. Starch: Uses of native starch. In C. Wrigley, H. Corke, K. Seetharaman, and F. Jon (Eds.), *Encyclopedia of Food Grains* (2nd ed., Vol. 3, pp. 274–281). Academic Press.

Li, J.-Y. and Yeh, A.-I. 2001. Relationships between thermal, rheological characteristics and swelling power for various starches. *Journal of Food Engineering* 50(3): 141–148.

Li, X., Wu, M., Xiao, M., Lu, S., Wang, Z., Yao, J. and Yang, L. 2019. Microencapsulated β-carotene preparation using different drying treatments. *Journal of Zhejiang University: Science B* 20(11): 901–909.

Liese, W. and Weiner, G. 1996. Ageing of bamboo culms. A review. *Wood Science and Technology*, 30(2): 77–89.

Littlewood, J., Wang, L., Turnbull, C. and Murphy, R.J. 2013. Techno-economic potential of bioethanol from bamboo in China. *Biotechnology for Biofuels* 6(1): 173.

Lopez-Rubio, A., Flanagan, B.M., Gilbert, E.P. and Gidley, M.J. 2008. A novel approach for calculating starch crystallinity and its correlation with double helix content: A combined XRD and NMR study. *Biopolymers* 89(9): 761–768.

Luo, J., Lian, C., Liu, R., Zhang, S., Yang, F. and Fei, B. 2019. Comparison of metaxylem vessels and pits in four sympodial bamboo species. *Scientific Reports* 9(1): 10876.

Marinopoulou, A., Christofilos, D., Arvanitidis, J. and Raphaelides, S.N. 2019. Study of molecular inclusion complex formation of amylose with indomethacin. *Starch* 71(7–8): 1800295.

Mateescu, M.A., Ispas-Szabo, P. and Assaad, E. (Eds.). (2015). Starch and derivatives as pharmaceutical excipients: From nature to pharmacy. In *Controlled Drug Delivery* (pp. 21–84). Woodhead Publishing.

Matsushima, R., Maekawa, M. and Sakamoto, W. 2015. Geometrical formation of compound starch grains in rice implements Voronoi diagram. *Plant and Cell Physiology*, 56(11): 2150–2157.

Maurer, H.W. 2009. Starch in the paper industry. In J. BeMiller and R. Whistler (Eds.), *Starch* (Third Edit, pp. 657–713). Academic Press.

Mistry, A.H., Schmidt, S.J., Eckhoff, S.R. and Sutherland, J.W. 1992. Alkali extraction of starch from corn flour. *Starch* 44(8): 284-288.

McGrance, S.J., Cornell, H.J. and Rix, C.J. 1998. A simple and rapid colorimetric method for the determination of amylose in starch products. *Starch* 50(4): 158–163.

Moorthy, S.N. 1991. Extraction of starches from tuber crops using ammonia. *Carbohydrate Polymers* 16(4): 391-398.

Ngobese, N.Z., Wokadala, O.C., Plessis, B.D., Da Silva, L.S., Hall, A., Lepule, S.P., Penter, M., Ngcobo, M.E.K. and Swart, H.C. 2018. Physicochemical and morphological properties of a small granule legume starch with atypical properties from wild mango (*Cordyla africana L.*) seeds: A comparison to maize, pea, and kidney bean starch. *Starch* 70(11–12): 1700345.

Núñez-Bretón, L.C., Cruz-Rodríguez, L.C., Tzompole-Colohua, M.L., Jiménez-Guzmán, J., Perea-Flores, M., Rosas-Flores, W. and González-Jiménez, F.E. 2019. Physicochemical, functional and structural characterization of Mexican Oxalis tuberosa starch modified by cross-linking. *Journal of Food Measurement and Characterization* 13: 2862-2870.

Ocampo-Salinas, I.O., Gómez-Aldapa, C.A., Castro-Rosas, J., Vargas-León, E.A., Guzmán-Ortiz, F.A., Calcáneo-Martínez, N. and Falfán-Cortés, R.N. 2020. Development of wall material for the microencapsulation of natural vanilla extract by spray drying. *Cereal Chemistry* 97(3): 555–565.

Paronen, P. And Juslin, M. 1983. Compressional characteristics of four starches. *Journal of Pharmacy and Pharmacology* 35(10): 627-635.

Preiss, J. 2018. Plant starch synthesis. In M. Sjöö and L. Nilsson (Eds.), *Starch in Food* (2nd ed., pp. 3–95). Woodhead Publishing.

Qi, X. and Tester, R.F. 2019. Starch granules as active guest molecules or microorganism delivery systems. *Food Chemistry* 271: 182–186.

Ramos da Silva, L., Piler de Carvalho, C.W., Velasco, J.I. and Fakhouri, F.M. 2020. Extraction and characterization of starches from pigmented rice. *International Journal of Biological Macromolecules* 156: 485-493.

Rahman, S.M., Wheatley, C. and Rakshit, S.K. 2003. Selection of sweet potato variety for high starch extraction. *International Journal of Food Properties* 6(3): 419-430.

Rocha, G.A., Fávaro-Trindade, C.S, and Grosso, C.R.F. 2012. Microencapsulation of lycopene by spray drying: Characterization, stability and application of microcapsules. *Food and Bioproducts Processing* 90(1): 37–42.

Rocha, T.S., Cunha, V.A.G., Jane, J. and Franco, C.M.L. 2011. Structural characterization of peruvian carrot (*Arracacia xanthorrhiza*) starch and the effect of annealing on its semicrystalline structure. *Journal of Agricultural and Food Chemistry* 59(8): 4208–4216.

Saifullah, M., Islam-Shishir, M.R., Ferdowsi, R., Tanver-Rahman, M.R. and Van-Vuong, Q. 2019. Micro and nano encapsulation, retention and controlled release of flavor and aroma compounds: A critical review. *Trends in Food Science & Technology*, 86: 230–251.

Sarko, A. and Wu, H.C.H. 1978. The crystal structures of A, B and C polymorphs of amylose and starch. *Starch* 30(3): 73–78.

Srichuwong, S., Sunarti, T., Mishima, T., Isono, N. and Hisamatsu, M. 2005. Starches from different botanical sources I: Contribution of amylopectin fine structure to thermal properties and enzyme digestibility. *Carbohydrate Polymers* 60(4): 529–538.

Tjahjadi, C. and Breene, W.M. 1984. Isolation and characterization of adzuki bean (*Vigna angularis cv* Takara) starch. *Journal of Food Science* 49(2): 558-562.

Tester, R.F., Karkalas, J. and Qi, X. 2004. Starch composition, fine structure and architecture. *Journal of Cereal Science* 39(2): 151–165.

Tian, Y., Yang, N., Li, Y., Xu, X., Zhan, J. and Jin, Z. 2010. Potential interaction between β-cyclodextrin and amylose-lipid complex in retrograded rice starch. *Carbohydrate Polymers* 80(2): 581–584.

Toledo, M.C.F., Azzini, A. and Reyes, F.G.R. 1987. Isolation and characterization of starch from bamboo culm (*Guadua flabellata*). Starch 39(5): 158–160.

Vamadevan, V. and Bertoft, E. 2015. Structure function relationships of starch components. *Starch* 67(1–2): 55–68.

Wang, S. and Copeland, L. 2013. Molecular disassembly of starch granules during gelatinization and its effect on starch digestibility: A review. *Food & Function* 4(11): 1564.

Waterschoot, J., Gomand, S.V., Fierens, E. and Delcour, J.A. 2015. Production, structure, physicochemical and functional properties of maize, cassava, wheat, potato and rice starches. *Starch* 67(1–2): 14–29.

Xie, Y.L., Jiang, W., Li, F., Zhang, Y., Liang, X.Y., Wang, M., Zhou, X., Wu, S.Y. and Zhang, C.H. 2020. Controlled release of spirotetramat using

starch-chitosan-alginate-encapsulation. *Bulletin of Environmental Contamination and Toxicology* 104(1): 149–155.

Ye, J., Hu, X., Luo, S., McClements, D.J., Liang, L. and Liu, C. 2018. Effect of endogenous proteins and lipids on starch digestibility in rice flour. *Food Research International* 106: 404–409.

Zaki-Rizkalla, C. M., Latif-Aziz, R. and Ibrahim-Soliman, I. 2013. Microencapsulation of hydroxyzine HCl by thermal phase separation: in vitro release enhancement and in vivo pharmacodynamic evaluation. *Pharmaceutical Development and Technology* 18(1): 196–209.

.